IEEE Access
Multidisciplinary ⋮ Rapid Review ⋮ Open Access Journal

Received 7 April 2025, accepted 13 May 2025, date of publication 23 May 2025, date of current version 9 June 2025.

Digital Object Identifier 10.1109/ACCESS.2025.3573072

RESEARCH ARTICLE

A Physics-Informed Machine Learning Framework for Permafrost Stability Assessment

POLINA PILYUGINA[1], TIMOFEY CHERNIKOV[2], MARIA SMIRNOVA[2], ALEXEY ZAYTSEV[1,3,4], ALEXANDER BULKIN[5,6,7], EVGENY BURNAEV[1,8], ILYA S. BELALOV[9], NAZAR SOTIRIADI[3], ALBERT EFIMOV[10], YURY MAXIMOV[11], (Senior Member, IEEE), AND OLEG ANISIMOV[12]

[1]Skolkovo Institute of Science and Technology, 143026 Moscow, Russia
[2]Moscow Institute of Physics and Technology, 141701 Moscow, Russia
[3]Sberbank of Russia PJSC, 117997 Moscow, Russia
[4]Beijing Institute of Mathematical Sciences and Applications, Beijing 101408, China
[5]International Center for Corporate Data Analysis, 38402 Saint Martin d'Hères, France
[6]Moscow State University, 119991 Moscow, Russia
[7]International Center for Corporate Data Analysis, Astana 631301, Kazakhstan
[8]Artificial Intelligence Research Institute (AIRI), 105064 Moscow, Russia
[9]FRC Biotechnology RAS, 117312 Moscow, Russia
[10]Sber Innovation and Research, Sberbank of Russia, 117312 Moscow, Russia
[11]Los Alamos National Laboratory, Los Alamos, NM 87545, USA
[12]State Hydrological Institute, 199004 St. Petersburg, Russia

Corresponding author: Alexander Bulkin (a.bulkin@skoltech.ru)

The work of Evgeny Burnaev and Alexey Zaytsev is supported by the Ministry of Economic Development of the Russian Federation (code 25-139-66879-1-0003).

ABSTRACT Global warming accelerates permafrost degradation, compromising the reliability of critical infrastructure relied upon by over five million people daily. Additionally, permafrost thaw releases substantial methane emissions due to the thawing of swamps, further amplifying global warming and climate change and thus posing a significant threat to more than eight billion people worldwide. To mitigate this growing risk, policymakers and stakeholders need accurate predictions of permafrost thaw progression. Comprehensive physics-based permafrost models often require complex, location-specific fine-tuning, making them impractical for widespread use. Although simpler models with fewer input parameters offer convenience, they generally lack accuracy. Purely data-driven models also face limitations due to the spatial and temporal sparsity of observational data. This work develops a physics-informed machine learning framework to predict permafrost thaw rates. By integrating a physics-based model into machine learning, the framework significantly enhances the feature set, enabling models to train on higher-quality data. This approach improves permafrost thaw rate predictions, supporting more reliable decision-making for construction and infrastructure maintenance in permafrost-vulnerable regions, with a forecast horizon spanning several decades.

INDEX TERMS Permafrost thaw, climate change, physics-informed machine learning framework.

I. INTRODUCTION

A defining characteristic of the Arctic environment is perennially frozen ground, or permafrost, which refers to any subsurface material that remains frozen for more than two consecutive years.

Permafrost occurs in diverse environments, including land, high mountain regions, and even the shelves of certain Arctic seas. Collectively, these three types of permafrost cover approximately one-quarter of the Northern Hemisphere's land surface, spanning around 16.7 million km^2 in Eurasia and 10.2 million km^2 in North America [1]; see Fig. 1 for further details.

Currently, permafrost underlies nearly 65% of Russia, 50% of Canada, and 15% of the United States, including about 80% of Alaska [2]. This region supports over 1,100 permafrost settlements [3], home to approximately five million people. A significant share of critical infrastructure is

The associate editor coordinating the review of this manuscript and approving it for publication was Jianquan Lu.

built on permafrost [4], including highways, railways, oil and gas pipelines, and nuclear power plants. The stability of these structures is increasingly threatened by permafrost thaw [3], [5], [6], [7], leading to increased risk for technological catastrophes.

Global warming leads to higher ground temperatures, promoting permafrost thaw and deepening the active layer. These changes negatively affect infrastructure stability by reducing the bearing capacity of building foundations [8], [9], [10], [11], widely supported by empirical evidence [8], [10], [11], [12].The economic consequences of permafrost thaw are substantial: the total direct cost of lost infrastructure in North America by the end of the 21st century is projected to exceed $5 billion [6], [7], [9], [12], [13], [14], [15], [16].

Furthermore, permafrost thaw contributes to the formation of gas emission craters, which release significant quantities of methane and other gases into the atmosphere [17], [18]. A particularly concerning phenomenon is the permafrost carbon feedback, where large carbon deposits stored in frozen soils are released during thawing, further exacerbating climate impacts on ecosystems [19], [20], [21], [22], [23].

Multiple factors influence permafrost dynamics, with active layer thickness (ALT) and mean annual ground temperature (MAGT) serving as key thaw indicators. The active layer, which thaws in summer and refreezes in winter, has a maximum seasonal thaw depth that defines ALT. While these thermal parameters are critical, other properties—such as soil texture, porosity, and excess ground ice content—also play a significant role in determining permafrost stability.

In this study, we define MAGT as the temperature at a depth where annual temperature fluctuations remain below 0.1° C. This operational definition is widely used to approximate permafrost thermal stability, though the measurement depth may vary depending on the study context.

A. GAP IN STATE-OF-THE-ART AND ITS IMPORTANCE

Developing a higher-fidelity model for mean annual ground temperature (MAGT) and active layer thickness (ALT) by combining domain-specific physics-based models with machine learning is the central focus of this paper. The complexity of permafrost physics and the limited availability of data make permafrost analysis particularly challenging.

Conventional physics-based studies on permafrost degradation typically link a limited set of climate parameters, primarily air temperature and precipitation, to ALT and MAGT. In contrast, AI/ML models can seamlessly incorporate additional complex information, such as soil and vegetation properties, complex landscape characteristics, and infrastructure development. However, machine learning models often have excessive data requirements unless they incorporate strong priors or domain knowledge [24].

In this paper, we explore the benefits of integrating physics-based models with machine learning algorithms, leading to arguably more robust and accurate predictions. Despite numerous studies on physics-informed machine learning in the broader context of climate risk assessment [25], [26], the problem of permafrost thaw has remained largely unexplored. Motivated by the challenges outlined above, this study is driven by the following research questions:

- **RQ1:** Does enriching a gradient-boosted tree model with analytic features from the Kudryavtsev equilibrium solution lower the prediction error for *both* mean-annual ground temperature (MAGT) and active-layer thickness (ALT) compared with a climate-only baseline?
- **RQ2:** How does the same hybrid model perform relative to the stand-alone Kudryavtsev model when driven by identical atmospheric forcing?

B. CONTRIBUTION: BRIDGING CRITICAL GAPS

This paper introduces a physics-informed machine learning approach for permafrost thaw prediction, addressing critical challenges posed by global warming. By integrating physics-based model outputs and key nonlinearities into machine learning, we enhance interpretability and overcome the data limitations of purely data-driven models. This fusion enables more accurate predictions of mean annual ground temperature and active layer thickness, crucial for assessing permafrost stability.

The key contributions of this paper are as follows:

- a robust and accurate prediction framework: our method seamlessly integrates physics-based permafrost models with machine learning, ensuring reliability through physical constraints;
- state-of-the-art accuracy: the combined approach significantly outperforms existing pure ML or pure physics models, improving permafrost thaw forecasts for better risk assessment;
- comprehensive empirical validation and uncertainty quantification: the model is rigorously validated with Circumpolar Active Layer Monitoring (CALM) data, incorporating uncertainty estimates for enhanced confidence.

The structure of this paper is as follows. The next section, ''State-of-the-Art,'' highlights key advances in permafrost modeling, including an exploration of existing physics-based models. Among these, one of the simplest yet most powerful, the Kudryavtsev model [27], is discussed in ''Materials and Methods,'' along with its integration into machine learning. The ''Data'' section provides a detailed description of the input data, which is crucial for machine learning performance. Finally, we present the empirical study results in the ''Results'' section.

II. STATE-OF-THE-ART: SURVEY

A. EXISTING METHODS

A comprehensive review of methodologies for permafrost modeling is presented in [28]. One class of models [29] integrates climatic parameters with variations in snow cover, vegetation, and soil properties. These models demonstrate strong alignment with observational data and have been

effectively applied in various contexts. For example, [9] employed such a model to evaluate geocryological risks arising from permafrost thawing. These physics-based models explicitly account for the thermophysical processes governing permafrost stability, providing a crucial baseline for assessing permafrost change.

Similarly, this approach simulates permafrost temperatures and the depth of the seasonally thawed layer [30]. Their study employed kriging to interpolate values over a spatial grid with a resolution of 0.25°. Predictive calculations are based on climate change projections from six Earth System Models in the CMIP5 (Coupled Model Intercomparison Project Phase 5), under the RCP 8.5 scenario, which assumes continued greenhouse gas emissions growth. Streletskiy et al. validate their results by comparing present-period predictions (2005-2015) with observational datasets before projecting changes for the mid-21st century (2050-2059). Unfortunately, the long-term stability of such extrapolations remains uncertain, as permafrost dynamics may be influenced by processes not fully captured in equilibrium-based models.

A different numerical approach based on statistical models is described in [14]. Hjort et al. calculated variables such as temperature, precipitation, organic carbon content, soil type, water body distribution, solar radiation, and topography for each point on a spatial grid. These variables, derived from CMIP5 climate scenarios, depend on greenhouse gas concentrations. Three IPCC scenarios (RCP 2.6, RCP 4.5, and RCP 8.5) are used to model these variables under different emissions pathways. The study employs four statistical models—generalized linear model (GLM), generalized additive model (GAM), random forest (RF), and generalized boosting model (GBM)—along with their ensemble. The resulting analysis produces a map of soil temperature and the thickness of the seasonally thawed layer. The prediction uncertainty of the ensemble model is estimated at ± 0.8°C for soil temperature and ± 0.4 m for the thawed layer thickness, highlighting both the potential and the limitations of purely statistical approaches in permafrost modeling.

A similar approach is explored in [31], with a greater emphasis on modeling procedures. This study reports root mean squared errors (RMSEs) of 0.5 m for active layer thickness (ALT) and 1.6Â°C for mean annual ground temperature (MAGT), evaluating on hindcast data for past periods. To date, this represents the highest reported precision in permafrost thaw prediction. However, a model with a ± 0.5 m prediction error remains insufficient for ensuring the stability and safety of infrastructure built over permafrost.

Recent results in [32] highlight the limitations of conventional machine learning methods in predicting environmental processes, including permafrost thaw, at high latitudes, particularly concerning carbon cycle balances. These findings suggest that empirical machine learning models, if not properly constrained by physical principles, may struggle with extrapolation to future climate scenarios beyond the training data distribution.

B. PHYSICS-INFORMED MODELING

In this study, we focus on incorporating the Kudryavtsev equilibrium model [27], [29], [33] into machine learning. Note that other models can be integrated into machine learning in a similar manner.

Equilibrium models suggest that the mean annual ground temperature (MAGT) is in balance with atmospheric parameters. These models have relatively low data requirements, often relying on mean monthly temperature and precipitation data as climate forcing, along with a few parameters characterizing soil thermal properties, snow, and vegetation. The equilibrium model developed by Kudryavtsev is one of the most successful examples [27]. With slight modifications, this model has been applied in numerous subsequent studies [9], [29], [30], [34], [35], [36].

Table 1 presents a comparative analysis of various models, all of which are compatible with the physics-informed machine learning (PIML) framework for permafrost degradation proposed in this paper. For clarity, however, we focus exclusively on the Kudryavtsev model in detail.

TABLE 1. Analytical/semi-analytical models for permafrost degradation that can be incorporated in the PIML framework of this paper.

Model	Predicts ALT?	Predicts MAGT?	PIML compatible?
Kudryavtsev et al. [40]	✓	✓	✓
TTOP [41], [42]	✗	✓	✓
Anisimov & Nelson [43]	✓	✗	✓
Jafarov et al. [44]	✓	✓	✓
Lunardini N-Factor [45]	✗	✓	✓
Ling & Zhang [46]	✓	✗	✓
Romanovsky & Osterkamp [47]	✓	✓	✓
Zhang et al. [48]	✓	✓	✓

Among the models listed in Table 1, we chose the Kudryavtsev model due to its well-established empirical grounding, analytical tractability, and compatibility with limited-input datasets. Unlike more complex transient models that often require detailed subsurface profiles and long-term calibration, the Kudryavtsev model can be robustly applied using readily available surface climate data. This makes it a practical and scalable choice for integration into a machine learning framework, particularly when operating under data scarcity constraints.

Despite recent improvements in MAGT and ALT data availability through a dedicated web portal [45], permafrost modeling remains constrained by limited data. More advanced transient models are often impractical due to missing input parameters and the inability to properly calibrate them. Given these challenges, we use the Kudryavtsev model not as a stand-alone predictor but as a feature generator within the PIML framework, ensuring that key physical processes are embedded in machine learning representations.

The Kudryavtsev model is based on a numerical solution of a nonlinear parabolic equation [27] and accounts for snow, vegetation, soil composition, and variable thermal

properties [33], [35]. It has been extensively validated against empirical observations [33].

In this model, each grid element (a pixel on the map) is associated with observable variables such as snow cover, vegetation, and soil characteristics. The model outputs ground temperature and active layer thickness. For this study, we used a modified version from [29]. A detailed description can be found in [28] and [29].

The model takes monthly air temperature and precipitation as climate inputs, along with various soil parameters. Instead of relying on a single model setup, we generate an ensemble of Kudryavtsev model outputs by varying key soil properties, specifically soil type (e.g., clay, loam, peat), while keeping snow cover and organic layer depth constant. This ensemble approach captures a range of plausible permafrost conditions, reducing sensitivity to single assumptions.

Snow cover is held constant to account for its dual role in ground heat exchange. It reflects solar radiation, helping to keep the ground cooler, while also acting as an insulator that slows both winter heat loss and summer heat gain, stabilizing temperature fluctuations. The organic layer depth is determined by the dominant vegetation type in each area.

III. MATERIALS AND METHODS

The core idea of physics-informed machine learning for permafrost thaw prediction is to enhance accuracy by combining advanced data-driven methods with physics-based models. Rather than using equilibrium models as standalone predictors, we incorporate their outputs as additional physical features in machine learning. This approach maintains consistency with known permafrost dynamics while improving the predictive power of data-driven techniques, enabling high-fidelity thaw predictions even with limited observational data.

The Circumpolar Active Layer Monitoring (CALM) program provides data from 265 sites across 15 countries in the Northern Hemisphere [46]. Figure 1 shows the locations of these sites. To assess permafrost degradation risks, we model seasonal thaw depth across the entire grid.

We trained several machine learning models using CALM site data. As often happens for data-limited problems, simple models like gradient boosting demonstrate substantially better performance than complex and highly non-linear methods. Inputs included dynamic climate parameters, static soil and vegetation data, and physical features derived from an ensemble of Kudryavtsev model outputs with varying parameter settings. Figure 2 illustrates the model workflow. The process begins by preprocessing input data, feeding it into the Kudryavtsev model [27], and using its outputs as additional features for the machine learning model.

A. PHYSICS-BASED MODEL

Physics-based models can be considered as coarse-grained approximators providing qualitative rather than quantitative description for permafrost thawing. Although even qualitative physics-based models can assist machine learning, leading to a proper feature space providing more informative process description thus facilitating prediction with machine learning methods.

The Kudryavtsev model, describing permafrost thaw from a heat flow equation perspective, is a vital example of the latter. The model is a solution to the equation of heat flow theory [28], described by (1).

$$C\frac{\delta T}{\delta t} = \lambda\frac{\delta^2 T}{\delta z^2} \tag{1}$$

where C is the effective volumetric heat capacity [J m^{-3}], T is temperature [K], t is time, λ is thermal conductivity [W $m^{-1}K^{-1}$] and z is the underground depth [m]. The thermal conductivity and the soil heat capacity are known for both train and test data.

The surface temperature can be considered as a leading-term approximation of the Fourier series:

$$T_s(t) \approx T_s + A_s \cos\left(\frac{2\pi t}{P}\right), \tag{2}$$

where $\bar{T}_s$ is a constant since climate change impact within a few years is considered being insignificant. The principal period P for temperature oscillations is one year, and A_s is an unknown (location-dependent) oscillation amplitude.

Based on the first principles, we assume that the depth of the oscillation magnitude decreases exponentially following the linear ordinary differential equation (ODE)

$$\frac{dA(z)}{dz} = -\beta, \quad A(z) = A_s \exp(-\beta z), \ \beta > 0. \tag{3}$$

Finally, since the temperature changes do not propagate immediately, we assume linear phase decay with the depth grow, which results in:

$$T(z,t) = T_s + A_s \exp(-\beta z)\cos\left(\frac{2\pi t}{P} - \gamma z\right) \tag{4}$$

Substituting the above Eqs. (2) – (4) in (1) and matching the derivatives we get

$$\beta = \gamma = \sqrt{\frac{\lambda\pi}{CP}}, \quad \lim_{z\to\infty} T(z,t) = T_s. \tag{5}$$

Notice that the MAGT we recover is simply T_s. The heat conservation law also implies that in the Kydryavtsev model the mean temperature averaged over a year does not change with depth.

Now, we derive the active layer thickness (ALT) as the solution to

$$0 = T(z_{thaw}, t) = T_s + A_s \exp^{-\beta z}\cos\left(\frac{2\pi t^*}{P} - \beta z_{thaw}\right) \tag{6}$$

where t^* stands for the warmest time of the year where $\cos(\cdot) = 1$. Thus, at the active layer thickness, z_{thaw}, we have

$$T_s + A_s \exp(-\beta z_{thaw}) = 0 \Rightarrow z_{thaw} = \frac{CP}{\lambda\pi}\ln\left(-\frac{T_s}{A_s}\right). \tag{7}$$

1) PHYSICS-BASED MODEL ASSISTANCE TO MACHINE LEARNING

The Kudryavtsev model essentially asserts that key permafrost parameters, MAGT and ALT, can be approximated as functions of annual average temperatures and their variations. These variations can be estimated using historical reanalysis data (ERA) and climate projections.

Specifically:

- Mean Annual Ground Temperature (MAGT), T_s: Defined as the average daily temperature over a year.
- Active Layer Thickness (ALT), z_{thaw} given by

$$z_{\text{thaw}} = \frac{CP}{\lambda\pi} \ln\left(-\frac{T_s}{A_s}\right), \tag{8}$$

where A_s is a robust estimate of the difference between maximum and minimum annual temperatures, Eq. (3).

This study demonstrates how incorporating the Kudryavtsev model as an additional feature set enhances machine learning-based permafrost thaw predictions. This integration is particularly valuable given the limited availability of permafrost observational data across both space and time. Moreover, more advanced models [28], [47], [48] could be integrated similarly to further refine prediction accuracy.

B. MACHINE LEARNING

To integrate physical constraints into our prediction framework, we first ran the Kudryavtsev model with various parameter initializations to generate ALT and MAGT values under different soil and climate conditions. These values are then used as inputs to a Machine Learning (ML) model along with other data, as described in the *Data* section. The ML model is subsequently trained and evaluated using historical observations from the CALM and TSP stations.

We use gridded climate data from an ensemble of CMIP6 Earth System Models to obtain predictions for the periods 2010–2015 and 2040–2060. The ML model is trained on present-day conditions and then applied to infer future permafrost states based on projected climate scenarios.

In the empirical part, we consider the two most notable greenhouse gas emission scenarios defined by the Shared Socioeconomic Pathways (SSP). SSP scenarios account for the impact of climate change on societal and economic development [49].

TABLE 2. Input data.

Input data	Parameters	Units	Period
IPA Permafrost Map	Permafrost type	Categorical	N/A
swamp	Swamp coverage	%	N/A
CEDA	Temperatures, precipitation	°C, mm	1901-2020
WorldClim (historical)	Temperature, precipitation	°C, mm	1960-2018
CALM	Thaw depth	cm	1969-2021 (partially)
WorldClim/CMIP6	Temperature, precipitation	°C, mm	2006-2100
vegetation	Type of vegetation	Categorical	N/A
GTNP-TSP	Temperature, zero-amplitude depth	°C, cm	1901-2020

C. DATA

The spatial resolution for historical data is 0.5 angular degrees, except for the GTNP-ALT dataset (see description below). For future predictions and historical assessments, we used high-resolution temperature and precipitation data from WorldClim [50], [51]. The temporal resolution of time series data ranged from 1 month to 1 year. We aggregate values of interest for each pixel using the datasets detailed below.

1) CEDA

Various climate variables [52], including cloud cover (average sky fraction obscured by clouds), daily temperature range, proportion of time with subzero temperatures, precipitation, monthly average daily minimum and maximum temperatures, monthly mean temperature, and proportion of time with precipitation. The temporal resolution is 1 month.

2) CALM

Thaw depth statistics [45] collected at CALM sites (Figure 1). Each data point includes eight entries: seven describe thaw depth characteristics (average, median, minimum, maximum, 25th percentile, 75th percentile, and standard deviation), and one represents the distance to the nearest CALM site. Measurements are taken on a 1 km × 1 km grid with 100-m steps (121 total points), though some data is missing or irregularly recorded. To standardize spatial resolution (0.5 angular degrees), we assigned each grid point to the nearest CALM site, with a maximum mapping distance of 200 km (four cases). The temporal resolution is 1 year. Missing values were ignored and not used for training or testing the approach.

3) WorldClim (HISTORICAL)

High-resolution historical climatic data is projected from CRU-TS-4.03 using WorldClim 2.1 for bias correction [50]. The data cover 1960-2018 with an original spatial resolution of 2.5 minutes (∼21 km^2), reprojected to a 0.5-angular-degree grid. The temporal resolution is 1 month.

4) IPA

Permafrost distribution map [53], rasterized from a vector format to 0.5 angular degrees for consistency with other datasets (Figure 1). These data are time-invariant.

5) WorldClim (CMIP6)

Climate projections from the CanESM5 model, including air temperature (mean, minimum, and maximum in °C) and precipitation (mm). The temporal resolution is 1 month [54].

6) SWAMP

Provided by Professor Oleg Anisimov, this dataset represents the percentage of wetlands for each grid point (Figure 2). These data are time-invariant.

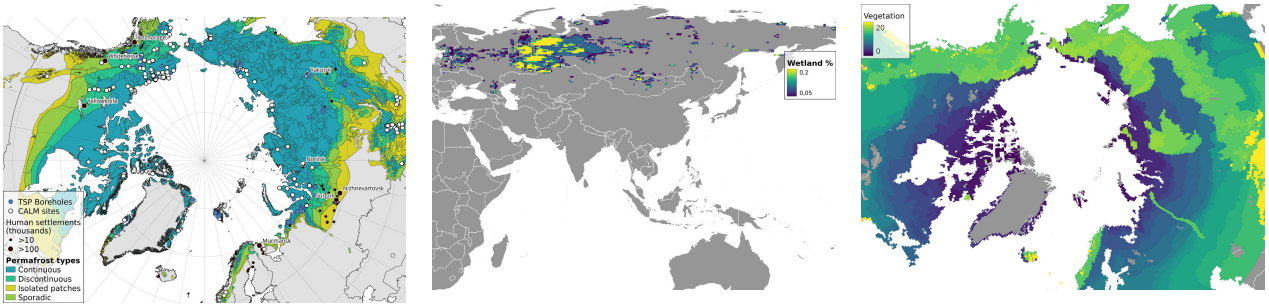

FIGURE 1. Left: distribution of permafrost types according to the IPA permafrost map with CALM sites and TSP boreholes. Center: wetland portion in each pixel. Right: vegetation portion in each pixel.

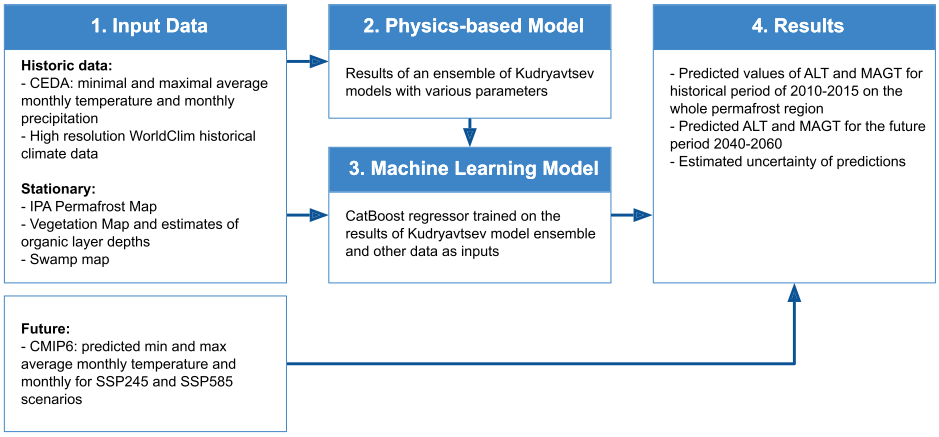

FIGURE 2. Model flowchart. Graphical summary of the methods section.

7) VEGETATION

Also provided by Professor Oleg Anisimov, this dataset classifies landscape types and biotopes (Figure 1). These data are time-invariant.

8) GTNP-TSP

Zero Annual Amplitude (ZAA) depth—where annual temperature variation is below 0.1°C [55]. These data describe permafrost thermal conditions measured at TSP boreholes (Figure 1). Since ZAA depth is not explicitly reported, we manually determined it for each weather station and year using GTNP data [45]. Stations lacking sufficient data for ZAA estimation are eliminated. The final dataset includes both ZAA temperature and depth, projected onto a regular grid to create a spatial map.

D. DATA FOR MODELING

Let $\mathcal{P}$ be the domain representing the part of the Earth's surface underlain by permafrost. We project this two-dimensional, locally continuous surface onto a discrete grid, $\mathbf{P}$, parameterized by two angular coordinates, i and j, with a step size of 0.5 degrees. For each grid cell at coordinates (i, j), we have observations of various features, $\vec{P}$, recorded at different time steps, τ, where the temporal resolution is 1 month. Thus, we define $\mathcal{P} \supset \mathbf{P} = \{\vec{P}_{ij}^{\tau}\}$ where each observation is indexed by both space and time.

The input data $\vec{P}$ for our model consists of dynamic climate variables (temperature and precipitation) and static parameters (swampiness, biotopes, and permafrost type):

$$\vec{P}_{ij}^{\tau} = \{i, j, \tau, X_{ij}^{\tau}, X_{ij}, Y_{ij}^{\tau}\} \tag{9}$$

where i, j are the latitude and longitude of the pixel center; τ is the year of observation; X_{ij}^{τ} contains 12 monthly values of climate variables (e.g., minimum and maximum temperatures, monthly precipitation); X_{ij} includes stationary parameters that do not vary over time (e.g., swampiness, biotopes, permafrost type); $Y_{ij}^{\tau} = \{alt_{ij}^{\tau}, magt_{ij}^{\tau}\}$ represents the observed ALT and MAGT values.

Our model takes X_{ij} and X_{ij}^{τ} as inputs. The key variables in this study, alt_{ij}^{τ} and $magt_{ij}^{\tau}$, are only recorded for a subset of the full grid $\mathbf{P}$. Consequently, we used this subset for training and validation.

E. IMPLEMENTATION

Our model incorporates both observed meteorological data and outputs from the Kudryavtsev model (see Fig. 2). The input data consist of 12 monthly measurements of temperature and precipitation, X_{ij}^{τ}, along with soil properties such as organic layer thickness and soil type, X_{ij}.

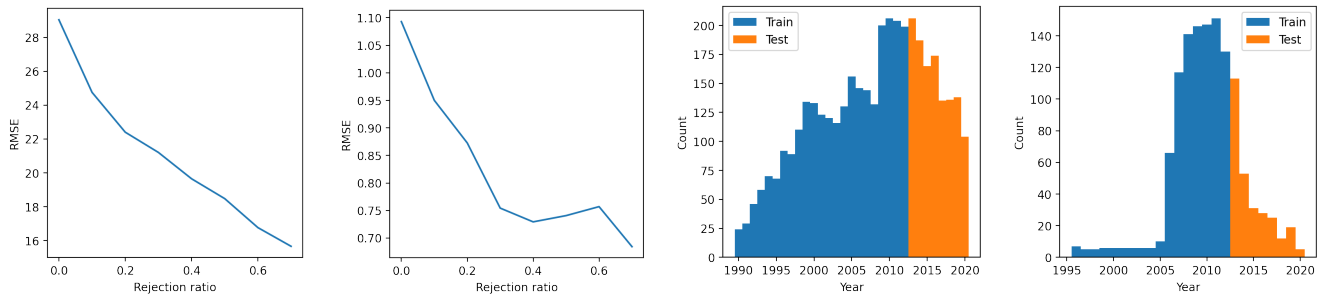

(a) Rejection curve for (active layer thickness)

(b) Rejection curve for (mean average ground temperature)

(c) Train-test split and number of observed ALT values

(d) Train-test split and number of observed MAGT values

FIGURE 3. Left: dependency of the error of the model on the test set alterations with dropping top k % (rejection ratio) values with the highest predictive uncertainty. Right: histograms of the number of observed ALT and MAGT values for a given year. The orange bars indicate the years used for the test.

TABLE 3. Mean annual ground temperatures (MAGT; left) and active layer thickness (ALT; right) prediction errors on the proposed training-testing splits. Each model is trained with 80% of the data and tested over the remaining. The average of five estimations for each model configuration is given. "Kudr." denotes the Kudryavtsev model results. The best results are in bold.

Model	Factors	RMSE Train	RMSE Test	$R^2 \times 100$ Train	$R^2 \times 100$ Test
CatBoost	All data	0.72 ± .11	**1.08** ± .02	89 ± 3	**53** ± 1
	Kudr. (ALT + MAGT)	1.04 ± .02	1.26 ± .02	77 ± 2	37 ± 2
	Kudr. (ALT)	1.27 ± .03	1.32 ± .01	67 ± 2	30 ± 1
	Kudr. (MAGT)	1.06 ± .08	1.22 ± .04	76 ± 3	41 ± 4
	Only climate data	0.64 ± .06	1.14 ± .02	91 ± 2	48 ± 2
Elastic Net	All data	1.24 ± .02	1.27 ± .03	68 ± 1	35 ± 3
	Kudr. (ALT + MAGT)	1.50 ± .02	1.25 ± .01	53 ± 1	38 ± 1
	Kudr. (ALT)	1.80 ± .04	1.50 ± .02	32 ± 1	10 ± 3
	Kudr. (MAGT)	1.61 ± .02	1.40 ± .01	46 ± 1	21 ± 1
	Only climate data	1.33 ± .02	1.55 ± .04	63 ± 1	4 ± 6
LinearRegression	All data	1.18 ± .02	1.41 ± .07	71 ± 1	20 ± 8
	Kudr. (ALT + MAGT)	1.42 ± .02	1.18 ± .02	58 ± 2	42 ± 2
	Kudr. (ALT)	1.55 ± .03	1.19 ± .01	50 ± 2	44 ± 1
	Kudr. (MAGT)	1.52 ± .02	1.17 ± .01	52 ± 1	45 ± 1
	Only climate data	1.29 ± .02	1.64 ± .05	65 ± 1	-7 ± 7
NeuralNetwork	All data	1.06 ± .07	1.56 ± .13	77 ± 3	2 ± 16
	Kudr. (ALT + MAGT)	1.41 ± .03	1.39 ± .05	59 ± 2	23 ± 5
	Kudr. (ALT)	1.50 ± .09	1.34 ± .01	53 ± 4	28 ± 1
	Kudr. (MAGT)	1.45 ± .05	1.35 ± .11	57 ± 2	27 ± 11
	Only climate data	1.05 ± .10	1.40 ± .23	77 ± 4	19 ± 26
RandomForest	All data	0.38 ± .01	1.16 ± .03	**97** ± 1	47 ± 2
	Kudr. (ALT + MAGT)	0.45 ± .02	1.24 ± .04	96 ± 1	38 ± 4
	Kudr. (ALT)	0.51 ± .02	1.41 ± .04	94 ± 1	21 ± 5
	Kudr. (MAGT)	0.48 ± .01	1.27 ± .04	95 ± 1	35 ± 4
	Only climate data	**0.37** ± .01	1.28 ± .08	97 ± 1	35 ± 8

Model	Factors	RMSE Train	RMSE Test	R^2 (×100) Train	R^2 (×100) Test
CatBoost	All data	**5.65** ± .90	**25.53** ± .40	**98** ± 1	**62** ± 1
	Kudr. (ALT + MAGT)	27.32 ± .55	32.39 ± .17	61 ± 2	38 ± 1
	Kudr. (ALT)	25.71 ± 1.69	36.71 ± .13	65 ± 5	21 ± 1
	Kudr. (MAGT)	27.41 ± 1.48	33.62 ± .54	60 ± 4	33 ± 2
	Only climate data	9.96 ± 1.63	28.57 ± .47	95 ± 2	52 ± 2
Elastic Net	All data	29.80 ± .31	37.79 ± .18	53 ± 1	16 ± 1
	Kudr. (ALT + MAGT)	38.93 ± .39	40.17 ± .18	20 ± 1	5 ± 1
	Kudr. (ALT)	39.79 ± .35	40.80 ± .39	17 ± 1	2 ± 2
	Kudr. (MAGT)	39.48 ± .40	39.96 ± .18	18 ± 1	6 ± 1
	Only climate data	31.14 ± .28	38.48 ± .27	49 ± 1	13 ± 1
LinearRegression	All data	28.48 ± .23	36.02 ± .23	57 ± 1	24 ± 1
	Kudr. (ALT + MAGT)	36.43 ± .27	39.76 ± .38	30 ± 1	7 ± 2
	Kudr. (ALT)	39.13 ± .38	40.76 ± .15	20 ± 1	2 ± 1
	Kudr. (MAGT)	38.23 ± .36	39.62 ± .33	23 ± 1	7 ± 2
	Only climate data	31.07 ± .28	38.93 ± .28	49 ± 1	11 ± 1
NeuralNetwork	All data	19.21 ± 1.30	29.53 ± .60	81 ± 3	49 ± 2
	Kudr. (ALT + MAGT)	33.50 ± .62	39.31 ± 1.88	41 ± 3	9 ± 9
	Kudr. (ALT)	38.65 ± .48	38.35 ± .31	21 ± 1	13 ± 1
	Kudr. (MAGT)	31.13 ± .94	36.73 ± .28	49 ± 3	21 ± 1
	Only climate data	17.81 ± 2.89	32.30 ± 1.14	83 ± 5	38 ± 4
RandomForest	All data	7.36 ± .12	29.57 ± .32	97 ± 1	48 ± 1
	Kudr. (ALT + MAGT)	10.43 ± .16	34.53 ± .26	94 ± 1	30 ± 1
	Kudr. (ALT)	12.89 ± .12	37.05 ± .16	91 ± 1	19 ± 1
	Kudr. (MAGT)	11.58 ± .28	35.03 ± .44	93 ± 1	28 ± 2
	Only climate data	7.62 ± .12	31.70 ± .28	97 ± 1	41 ± 1

To parameterize the Kudryavtsev model, we varied soil type configurations. The model initialization includes parameters for four soil types: sand, loam, clay, and peat. The dominant soil type in permafrost regions is clay, which shares similar physicochemical properties with loam. Therefore, we obtained model predictions for both soil types. Additionally, to account for hydrological variability, we generated predictions for both dry and wet soil conditions. For swamp-associated locations, we computed a weighted average of the regular soil type and peat predictions based on the *swamp* dataset (see Fig. 1). As a result, each pixel had four pairs of ALT and MAGT values to initialize the Kudryavtsev model.

Our machine learning model finally predicts alt_{ij}^{τ} and $magt_{ij}^{\tau}$ by leveraging both environmental predictors, $\vec{P}_{ij}^{\tau} \in \mathbf{P}_{alt}$, and the Kudryavtsev model outputs from the previous step.

To evaluate performance and select the most suitable model, we experimented with various machine learning techniques, including linear [56], multi-layer perceptron [57], random forest [58], elastic net [59], and CatBoost regressions [60]

Based on prediction errors, we selected CatBoost Regressor [60] as the most reliable method. This model is a supervised learning meta-algorithm that constructs an ensemble of decision trees, reducing bias and variance to improve prediction quality. It offers built-in parallelization, enabling fast training and inference on a standard laptop.

For uncertainty estimation, we used built-in algorithms in CatBoost. Specifically, we trained the model with a specialized loss function that enables uncertainty estimation via virtual ensembles, following the approach in [61]. Additionally, we provided rejection curves for estimated uncertainty values by systematically removing data points with the highest predictive uncertainty, see Fig. 3 for details. For engineering use, the 95 % upper ALT bound may be read as a conservative foundation depth.

The goal of our model is to provide robust predictions of permafrost degradation under future climate scenarios.

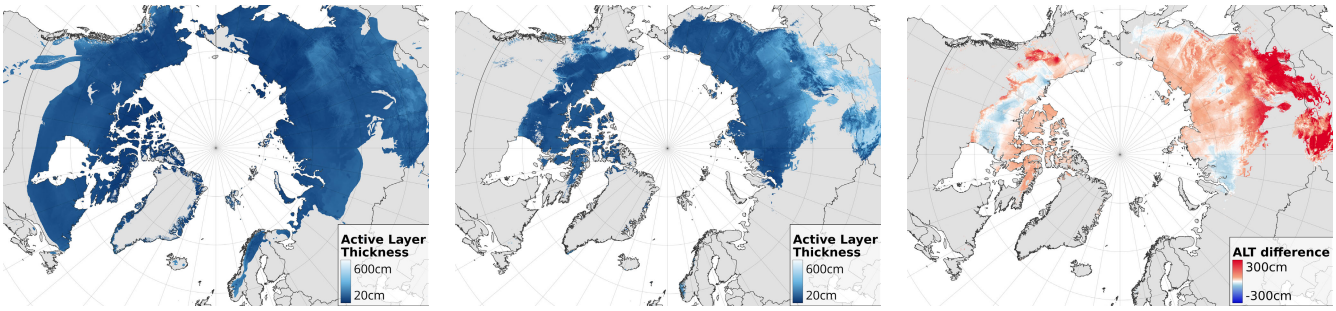

(a) Active layer thickness (ALT), 2010 (b) Active layer thickness (ALT), 2050 (c) ALT difference between 2050 and 2010

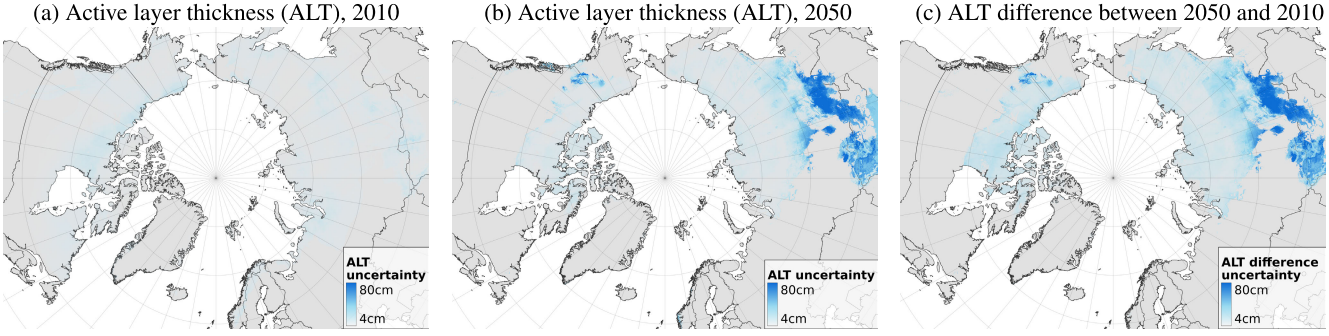

(d) Active layer thickness (ALT) uncertainty, 2010 (e) Active layer thickness (ALT) uncertainty, 2050 (f) ALT difference uncertainty between 2050 and 2010

FIGURE 4. Comparison of the active layer thickness in 2010 and 2050 under the CMIP6 SSP245 scenario.

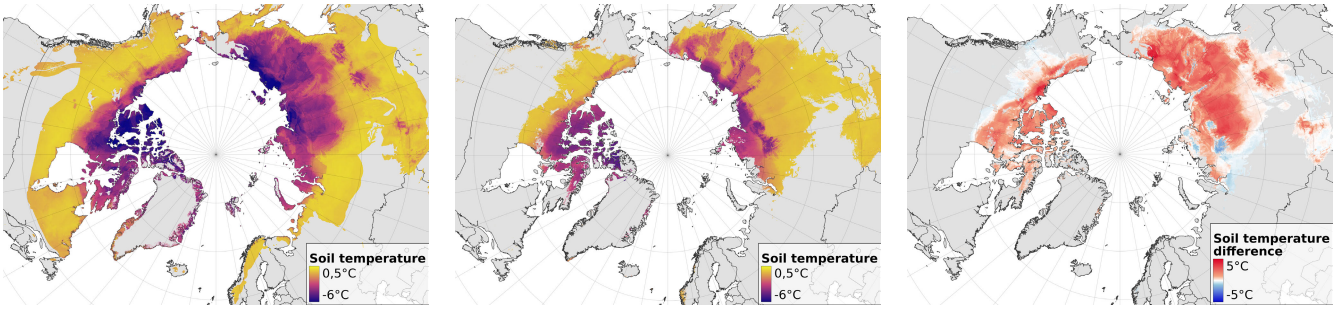

(a) Temperature, 2010 (b) Temperature, 2050 (c) Temperature difference, 2050 and 2010

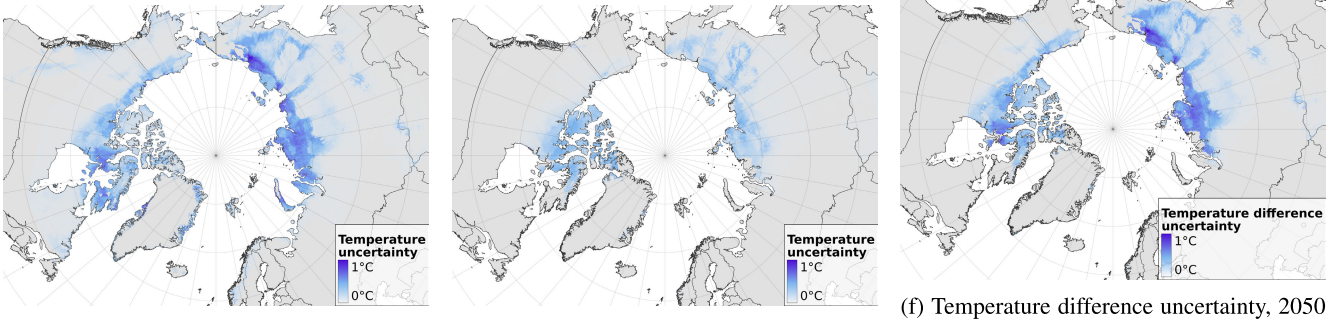

(d) Temperature uncertainty, 2010 (e) Temperature uncertainty, 2050 (f) Temperature difference uncertainty, 2050 and 2010

FIGURE 5. Comparison of the mean annual ground temperature at zero amplitude in 2010 and 2050 under the CMIP 6 SSP245 scenario.

To achieve this, we replace historical climate data with projected temperature and precipitation from the CMIP6 Earth System Model ensemble, ensuring that future projections reflect the latest climate pathways. Consequently, the Kudryavtsev model outputs are updated using CMIP6-based forcing data.

IV. RESULTS

In total, we used 2,729 ALT and 961 MAGT data points collected between 1990 and 2010, covering areas of 364,000 km^2 and 322,000 km^2, respectively. These data points correspond to map pixels that contain or neighbor CALM sites and/or TSP boreholes.

To evaluate model performance and assess its ability to predict future values, we divided the dataset into training and test subsets. The training set included data up to 2013, while the test set covered the period from 2013 to 2020. This temporal split ensures that the model is tested on a distinct time period, allowing us to assess its generalization to new conditions. Figure 3 illustrates an example of the training-testing split used. Additionally, we applied the K-fold algorithm to further partition the training set into five folds, each containing 80% of randomly selected data points.

Table 3 presents prediction errors for different models constructed using four sets of climate variables, with and without the Kudryavtsev model outputs. We evaluate model performance using two key metrics: root mean square error (RMSE) [62] and the coefficient of determination (R^2) [63].

The RMSE for the Kudryavtsev model alone (without additional climate data) is 32.39 $\pm$ 0.17 cm for ALT and 1.26 $\pm$ 0.02 for MAGT. While this serves as a strong baseline, it highlights the limitations of using an equilibrium model in isolation. Incorporating all available climate and environmental data into our physics-informed ML framework significantly improved test RMSE, reducing it to 25.53 $\pm$ 0.40 cm for ALT and 1.08 $\pm$ 0.02 for MAGT. These results demonstrate the added value of combining physical models with machine learning.

Figure 4 (a,d) and 5 (a,d) shows the predicted values by the CatBoost model, which is trained with all factors included *versus* the actual active layer thickness computed using all climatic data in the "Data" section. Although our model demonstrates excellent predictive power, it slightly underestimates the ALT.

Figures 4 (b,c,e,f) and 5 (b,c,e,f) demonstrate the predicted active layer thickness and temperature of the soil at the zero-amplitude level for 2050 (under the CMIP 6 SSP245 scenario) and as a comparison to 2010.

While direct benchmarking against prior permafrost models is limited due to variations in input data and spatial scales, we note that our model achieves competitive or superior performance. For instance, the RMSE of 25.5 cm for ALT prediction compares favorably with the $\pm$40 cm reported by Hjort et al. [4], [14] and the 0.5 m error [31]. These results highlight the efficacy of our physics-informed approach, especially when evaluated on an independent test period.

V. CONCLUSION

This study presents a physics-informed machine learning framework for predicting permafrost degradation with improved accuracy and robustness. By integrating the physics-based model (Kudryavtsev model in particular) into data-driven predictions, we overcome the limitations of purely empirical or physics-only approaches. Our model demonstrates strong generalization to future climate scenarios and outperforms existing methods in key metrics. This approach not only improves predictive fidelity, but also provides a scalable tool for long-term risk assessment in Arctic infrastructure planning and climate policy. Next steps for the research could include assimilating higher-resolution snow, vegetation, and soil-property datasets, and evaluating alternative equilibrium thaw-depth formulations beyond the Kudryavtsev model within the same hybrid architecture.

REFERENCES

[1] J. Obu, "How much of the Earth's surface is underlain by permafrost?" *J. Geophys. Res., Earth Surf.*, vol. 126, no. 5, pp. 1–5, May 2021.

[2] O. J. Ferrians, "Permafrost in Alaska," *Geol. North Amer.*, vol. 1, pp. 845–854, Apr. 2015.

[3] J. Ramage, L. Jungsberg, S. Wang, S. Westermann, H. Lantuit, and T. Heleniak, "Population living on permafrost in the Arctic," *Population Environ.*, vol. 43, no. 1, pp. 22–38, Sep. 2021.

[4] J. Hjort, D. Streletskiy, G. Doré, Q. Wu, K. Bjella, and M. Luoto, "Impacts of permafrost degradation on infrastructure," *Nature Rev. Earth Environ.*, vol. 3, no. 1, pp. 24–38, Jan. 2022.

[5] D. Reimchen, G. Doré, D. Fortier, and R. Walsh, "Cost and constructability of permafrost test sections along the Alaska highway, Yukon," in *Proc. Annu. Conf. Exhib. Transp. Assoc. Canada-Transp. Climate Change*, Jan. 2009, pp. 1–18.

[6] P. Larsen, S. Goldsmith, O. Smith, M. Wilson, K. Strzepek, P. Chinowsky, and B. Saylor, "Estimating future costs for Alaska public infrastructure at risk from climate change," *Global Environ. Change*, vol. 18, no. 3, pp. 442–457, Aug. 2008.

[7] A. M. Melvin, P. Larsen, B. Boehlert, J. E. Neumann, P. Chinowsky, X. Espinet, J. Martinich, M. S. Baumann, L. Rennels, A. Bothner, D. J. Nicolsky, and S. S. Marchenko, "Climate change damages to Alaska public infrastructure and the economics of proactive adaptation," *Proc. Nat. Acad. Sci. USA*, vol. 114, no. 2, pp. E122–E131, Jan. 2017.

[8] O. A. Anisimov, V. Kokorev, D. A. Streletskiy, and N. Shiklomanov, "Assessment report the main natural and socio-economic consequences of climate change in permafrost areas: A forecast based upon a synthesis of observations and modelling," Greenpeace USA, Washington, DC, USA, Assessment 2014.

[9] OA Anisimov and D Streletskiy, "Geocryological hazards of thawing permafrost," *Arctika XXI Century*, vol. 2, pp. 60–74, Jun. 2015.

[10] D. Streletskiy, O. Anisimov, and A. Vasiliev, "Permafrost degradation," in *Snow and Ice-Related Hazards, Risks, and Disasters*. Cham, Switzerland: Springer, Dec. 2015.

[11] D. A. Streletskiy, A. B. Sherstiukov, O. W. Frauenfeld, and F. E. Nelson, "Changes in the 1963–2013 shallow ground thermal regime in Russian permafrost regions," *Environ. Res. Lett.*, vol. 10, no. 12, Dec. 2015, Art. no. 125005.

[12] D. Streletskiy, "Permafrost degradation," in *Snow and Ice-Related Hazards, Risks, and Disasters*, Feb. 2021, pp. 297–322.

[13] B. Porfiriev, S. Voronina, V. Semikashev, N. Terentiev, D. Eliseev, and Y. Naumova, "Climate change impact on economic growth and specific sectors' development of the Russian Arctic," *Arcti, Ecol. Economy*, vol. 4, no. 28, pp. 4–17, Dec. 2017.

[14] J. Hjort, O. Karjalainen, J. Aalto, S. Westermann, V. E. Romanovsky, F. E. Nelson, B. Etzelmuller, and M. Luoto, "Degrading permafrost puts Arctic infrastructure at risk by mid-century," *Nature Commun.*, vol. 9, no. 1, pp. 1–16, Dec. 2018.

[15] N. I. Shiklomanov, D. A. Streletskiy, T. B. Swales, and V. A. Kokorev, "Climate change and stability of urban infrastructure in Russian permafrost regions: Prognostic assessment based on GCM climate projections," *Geographical Rev.*, vol. 107, no. 1, pp. 125–142, Jan. 2017.

[16] S. V. Badina, "Estimation of the value of buildings and structures in the context of permafrost degradation: The case of the Russian Arctic," *Polar Sci.*, vol. 29, Sep. 2021, Art. no. 100730.

[17] V. Bogoyavlensky, "The threat of catastrophic gas emissions from the Arctic permafrost zone," *Funnels Yamal Taymyr. Drill. Oil*, vol. 10, pp. 4–8, Aug. 2014.

[18] A. N. Khimenkov, D. O. Sergeev, Y. V. Stanilovskaya, A. N. Vlasov, D. B. Volkov-Bogorodsky, V. P. Merzlyakov, and G. S. Tipenko, "Structural transformations of permafrost before the formation of the yamal craters," in *Natural Hazards and Risk Research in Russia*. Cham, Switzerland: Springer, 2019, pp. 305–316.

[19] S. M. Natali et al., "Large loss of CO_2 in winter observed across the northern permafrost region," *Nature Climate Change*, vol. 9, no. 11, pp. 852–857, Oct. 2019.

[20] E. A. G. Schuur, A. D. McGuire, C. Schädel, G. Grosse, J. W. Harden, D. J. Hayes, G. Hugelius, C. D. Koven, P. Kuhry, D. M. Lawrence, S. M. Natali, D. Olefeldt, V. E. Romanovsky, K. Schaefer, M. R. Turetsky, C. C. Treat, and J. E. Vonk, "Climate change and the permafrost carbon feedback," *Nature*, vol. 520, no. 7546, pp. 171–179, Apr. 2015.

[21] L. Mattsson and O. A. Anisimov, "Potential feedback of thawing permafrost to the global climate system through methane emission," *Environ. Res. Lett.*, vol. 2, no. 4, Oct. 2007, Art. no. 045016.

[22] T. R. Christensen, T. Johansson, H. J. Åkerman, M. Mastepanov, N. Malmer, T. Friborg, P. Crill, and B. H. Svensson, "Thawing sub-Arctic permafrost: Effects on vegetation and methane emissions," *Geophys. Res. Lett.*, vol. 31, no. 4, pp. 1–18, Feb. 2004.

[23] K. R. Miner, M. R. Turetsky, E. Malina, A. Bartsch, J. Tamminen, A. D. McGuire, A. Fix, C. Sweeney, C. D. Elder, and C. E. Miller, "Permafrost carbon emissions in a changing Arctic," *Nature Rev. Earth Environ.*, vol. 3, no. 1, pp. 55–67, Jan. 2022.

[24] P. Niyogi, F. Girosi, and T. Poggio, "Incorporating prior information in machine learning by creating virtual examples," *Proc. IEEE*, vol. 86, no. 11, pp. 2196–2209, 1998.

[25] K. Kashinath et al., "Physics-informed machine learning: Case studies for weather and climate modelling," *Phil. Trans. Roy. Soc. A, Math., Phys. Eng. Sci.*, vol. 379, no. 2194, Apr. 2021, Art. no. 20200093.

[26] L. Zhong, H. Lei, and B. Gao, "Developing a physics-informed deep learning model to simulate runoff response to climate change in Alpine catchments," *Water Resour. Res.*, vol. 59, no. 6, Jun. 2023, Art. no. e2022WR034118.

[27] V. A. Kudryavtsev, L. S. Garagulya, and V. G. Melamed, "Fundamentals of frost forecasting in geological engineering investigations," Cold Regions Res. Eng. Lab., Hanover, NH, USA, Tech. Rep., 1977.

[28] D. Riseborough, N. Shiklomanov, B. Etzelmuller, S. Gruber, and S. Marchenko, "Recent advances in permafrost modelling," *Permafrost Periglacial Processes*, vol. 19, no. 2, pp. 137–156, Apr. 2008.

[29] O. A. Anisimov, "Verojatnostno-statisticheskoe modelirovanie moshhnosti sezonno-talogo sloja V uslovijah sovremennogo I budushhego klimata," *Kriosfera Zemli*, vol. 3, no. 3, pp. 36–44, 2016.

[30] D. A. Streletskiy, L. Suter, N. I. Shiklomanov, B. N. Porfiriev, and D. O. Eliseev, "Assessment of climate change impacts on buildings, structures and infrastructure in the Russian regions on permafrost," *Environ. Res. Lett.*, vol. 14, no. 2, Feb. 2019, Art. no. 025003.

[31] J. Aalto, O. Karjalainen, J. Hjort, and M. Luoto, "Statistical forecasting of current and future Circum-Arctic ground temperatures and active layer thickness," *Geophys. Res. Lett.*, vol. 45, no. 10, pp. 4889–4898, May 2018.

[32] I. A. Shirley, Z. A. Mekonnen, R. F. Grant, B. Dafflon, and W. J. Riley, "Machine learning models inaccurately predict current and future high-latitude C balances," *Environ. Res. Lett.*, vol. 18, no. 1, Jan. 2023, Art. no. 014026.

[33] N. I. Shiklomanov and F. E. Nelson, "Analytic representation of the active layer thickness field, kuparuk river basin, Alaska," *Ecol. Model.*, vol. 123, nos. 2–3, pp. 105–125, Nov. 1999.

[34] E. E. Jafarov, S. S. Marchenko, and V. E. Romanovsky, "Numerical modeling of permafrost dynamics in Alaska using a high spatial resolution dataset," *Cryosphere*, vol. 6, no. 3, pp. 613–624, Jun. 2012.

[35] T. S. Sazonova and V. E. Romanovsky, "A model for regional-scale estimation of temporal and spatial variability of active layer thickness and mean annual ground temperatures," *Permafrost Periglacial Processes*, vol. 14, no. 2, pp. 125–139, Apr. 2003.

[36] D. A. Streletskiy, N. I. Shiklomanov, and V. I. Grebenets, "Changes of foundation bearing capacity due to climate warming in Northwest Siberia," *Earth's Cryosphere*, vol. 16, no. 1, pp. 22–32, 2012.

[37] K. Wang, E. Jafarov, and I. Overeem, "Sensitivity evaluation of the kudryavtsev permafrost model," *Sci. Total Environ.*, vol. 720, Jun. 2020, Art. no. 137538.

[38] F. E. Nelson and S. I. Outcalt, "A computational method for prediction and regionalization of permafrost," *Arctic Alpine Res.*, vol. 19, no. 3, pp. 279–288, Aug. 1987.

[39] J. Obu et al., "Northern Hemisphere permafrost map based on TTOP modelling for 2000–2016 at 1 km2 scale," *Earth-Sci. Rev.*, vol. 193, pp. 299–316, Apr. 2019.

[40] O. A. Anisimov and F. E. Nelson, "Permafrost distribution in the northern Hemisphere under scenarios of climatic change," *Global Planet. Change*, vol. 14, nos. 1–2, pp. 59–72, Aug. 1996.

[41] V. J. Lunardini, "Climatic warming and the degradation of warm permafrost," *Permafrost Periglacial Processes*, vol. 7, no. 4, pp. 311–320, Oct. 1996.

[42] F. Ling and T. Zhang, "Impact of the timing and duration of seasonal snow cover on the active layer and permafrost in the Alaskan Arctic," *Permafrost Periglacial Processes*, vol. 14, no. 2, pp. 141–150, Apr. 2003.

[43] V. E. Romanovsky and T. E. Osterkamp, "Thawing of the active layer on the coastal plain of the Alaskan Arctic," *Permafrost Periglacial Processes*, vol. 8, no. 1, pp. 1–22, Jan. 1997.

[44] Y. Zhang, X. Wang, R. Fraser, I. Olthof, W. Chen, D. Mclennan, S. Ponomarenko, and W. Wu, "Modelling and mapping climate change impacts on permafrost at high spatial resolution for an Arctic region with complex terrain," *Cryosphere*, vol. 7, no. 4, pp. 1121–1137, Jul. 2013.

[45] B. K. Biskaborn, J.-P. Lanckman, H. Lantuit, K. Elger, D. A. Streletskiy, W. L. Cable, and V. E. Romanovsky, "The new database of the global terrestrial network for permafrost (GTN-P)," Tech. Rep., 2015.

[46] N. Shiklomanov and G. Washington, "The circumpolar active layer monitoring (CALM) program: Data collection, management, and dissemination strategies informal roads: The impact of unofficial transportation routes on remote Arctic communities view project Arctic pire view project dmitry a streletskiy," Tech. Rep.

[47] C. D. Koven, W. J. Riley, and A. Stern, "Analysis of permafrost thermal dynamics and response to climate change in the CMIP5 Earth system models," *J. Climate*, vol. 26, no. 6, pp. 1877–1900, Mar. 2013.

[48] O. A. Anisimov, N. I. Shiklomanov, and F. E. Nelson, "Variability of seasonal thaw depth in permafrost regions: A stochastic modeling approach," *Ecol. Model.*, vol. 153, no. 3, pp. 217–227, Aug. 2002.

[49] K. Riahi et al., "The shared socioeconomic pathways and their energy, land use, and greenhouse gas emissions implications: An overview," *Global Environ. Change*, vol. 42, pp. 153–168, Sep. 2016.

[50] S. E. Fick and R. J. Hijmans, "WorldClim 2: New 1-km spatial resolution climate surfaces for global land areas," *Int. J. Climatol.*, vol. 37, no. 12, pp. 4302–4315, Oct. 2017.

[51] I. Harris, P. D. Jones, T. J. Osborn, and D. H. Lister, "Updated high-resolution grids of monthly climatic observations – the CRU TS3.10 dataset," *Int. J. Climatol.*, vol. 34, no. 3, pp. 623–642, Mar. 2014.

[52] I. C. Harris, P. D. Jones, and T. Osborn, "CRU ts4. 01: Climatic research unit (CRU) time-series (TS) version 4.01 of high-resolution gridded data of," Centre for Environ. Data Anal., Didcot, U.K., Tech. Rep., 2017.

[53] J. Brown, O. Ferrians, J. A. Heginbottom, and E. Melnikov, "Circum–Arctic map of permafrost and ground-ice conditions," Tech. Rep., 2002.

[54] World Climate Res. Programme. (2025). *Coupled Model Interconnection Project*. [Online]. Available: https://www.wcrp-climate.org/wgcm-cmip/wgcm-cmip6

[55] V. E. Romanovsky, S. L. Smith, and H. H. Christiansen, "Permafrost thermal state in the polar northern Hemisphere during the international polar year 2007–2009: A synthesis," *Permafrost Periglacial Processes*, vol. 21, no. 2, pp. 106–116, Apr. 2010.

[56] F. Galton, "Regression towards mediocrity in hereditary stature," *J. Anthropol. Inst. Great Britain Ireland*, vol. 15, p. 246, Jan. 1886.

[57] G. E. Hinton, "Connectionist learning procedures," in *Machine Learning*. Amsterdam, The Netherlands: Elsevier, 1990, pp. 555–610.

[58] L. Breiman, "Random forests," *Mach. Learn.*, vol. 45, no. 1, pp. 5–32, 2001.

[59] H. Zou and T. Hastie, "Regularization and variable selection via the elastic net," *J. Roy. Stat. Soc. Ser. B, Stat. Methodol.*, vol. 67, no. 2, pp. 301–320, Apr. 2005.

[60] L. Prokhorenkova, G. Gusev, A. Vorobev, A. V. Dorogush, and A. Gulin, "CatBoost: Unbiased boosting with categorical features," in *Proc. Adv. Neural Inf. Process. Syst.*, vol. 31, Dec. 2018, pp. 6639–6649.

[61] A. Ustimenko, L. Prokhorenkova, and A. Malinin, "Uncertainty in gradient boosting via ensembles," in *Proc. Int. Conf. Learn. Represent.*, Jan. 2020, pp. 1–14.

[62] J. S. Armstrong and F. Collopy, "Error measures for generalizing about forecasting methods: Empirical comparisons," *Int. J. Forecasting*, vol. 8, no. 1, pp. 69–80, Jun. 1992.

[63] R. A. Fisher, "On the probable error of a coefficient of correlation deduced from a small sample," *Metron*, vol. 1, pp. 1–32, Jan. 1921.

POLINA PILYUGINA received the M.Sc. degree in mathematics and computer science from the Skolkovo Institute of Science and Technology (Skoltech), in 2020, where she is currently pursuing the Ph.D. degree in computational and data science and engineering. Her main research interests include time series forecasting and classification, automated machine learning, topological data analysis, and physics-informed machine learning.

TIMOFEY CHERNIKOV received the B.Sc. degree in mathematics and computer science from Moscow Institute of Physics and Technology (MIPT). At Skoltech, he conducted research on time series forecasting. He is currently a Quantitative Researcher in finance, with a focus on data-driven modeling, statistical analysis, and algorithmic trading strategies.

MARIA SMIRNOVA is currently pursuing the B.Sc. degree in applied mathematics and physics with Moscow Institute of Physics and Technology. Her main research interests include climate change prediction, physical systems modeling, and physics-informed machine learning.

ALEXEY ZAYTSEV received the degree from MIPT, in 2012, and the Ph.D. degree from IITP RAS, in 2017. He is currently an Associate Professor with the Skolkovo Institute of Science and Technology. His research interests include machine learning and deep learning, specifically the development of new methods for sequential data and uncertainty estimation.

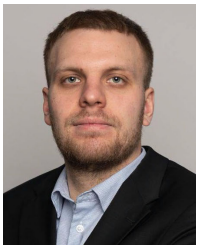

ALEXANDER BULKIN received the degree from the Department of Mathematics and Mechanics, Moscow State University, in 2020. He is currently pursuing the Ph.D. degree with the Department of Mathematics and Mechanics, Skolkovo Institute of Science and Technology. He is a Team Leader with the Skolkovo Institute of Science and Technology, working on the impact of climate change impact to the financial markets.

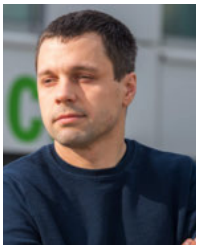

EVGENY BURNAEV received the M.Sc. degree in applied physics and mathematics from Moscow Institute of Physics and Technology, in 2006, the Ph.D. degree in foundations of computer science from the Institute for Information Transmission Problem RAS, in 2008, and the Dr.Sci. degree in mathematical modeling and numerical methods from Moscow Institute of Physics and Technology. He is currently the Director of the AI Center, Skolkovo Institute of Science and Technology, and a Full Professor. His research interests include generative modeling, manifold learning, deep learning for 3D data analysis, multi-agent systems, and industrial applications.

ILYA S. BELALOV received the Diploma degree in biochemistry from Moscow State University, in 2008, the Ph.D. degree in virology from the Institute of Poliomyelitis, in 2011, the M.Sc. degree in political science from HSE University, in 2017, and the B.Sc. degree in metric geometry from Moscow State University, in 2023. He is currently working in mathematical biology and bioinformatics at the FRC Biotechnology RAS, occasionally invading new research areas.

NAZAR SOTIRIADI received the master's degree in environmental science from Moscow State University. He is currently the Head of the ESG Risk Department, Sberbank of Russia. He has worked on several industrial ecology and climate projects.

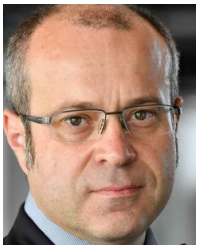

ALBERT EFIMOV received the degree in applied mathematics from Moscow Institute of Radio Engineering, Electronics and Automation, in 1993, and the M.S. degree in communications management from the University of Strathclyde, in 2003. Since 2017, he has been the Head of the Robotics Laboratory, Sberbank of Russia, where he is currently the Vice President and the Director of the Research and Innovation Department of the Technology Block. He is the author of publications on the Russian innovation ecosystem, robotics, and artificial intelligence.

YURY MAXIMOV (Senior Member, IEEE) received the B.S. and Ph.D. degrees in applied mathematics and control from Moscow Institute of Physics and Technology. From 2013 to 2014, he was a Postdoctoral Researcher with INRIA and the University of Grenoble Alpes. He joined Los Alamos National Laboratory, as a Staff Member, in 2016. He is the author of more than 70 articles in computer science, engineering, and applied mathematics.

OLEG ANISIMOV is currently a Professor of physical geography with the State Hydrological Institute, St. Petersburg, Russia. He was the coordinating lead author of the Polar regions chapters in the Third, Fourth, and Fifth IPCC reports, and the lead author of the international scientific assessments focused on the Arctic (ACIA, SWIPA). His research interests include environmental and socioeconomic impacts of changing climate in the northern lands.